Electrical conductivity of the ionic conductor tetragonal $(Bi_2O_3)_{1-x}(Eu_2O_3)_x$

(Condutividade elétrica do condutor iônico $(Bi_2O_3)_{1-x}(Eu_2O_3)_x$ tetragonal)

S. Yilmaz[1], O. Turkoglu[2], M. Ari[1], I. Belenli[3]
[1]Department of Physics, Mersin University, Mersin 33000, Turkey
[2]Department of Chemistry, Erciyes University, Kayseri 38039, Turkey
[3]Department of Physics, Abant Izzet Baysal University, Bolu 14280, Turkey
yilmazsr@gmail.com

Abstract

Electrical conductivity of tetragonal β-phase $(Bi_2O_3)_{1-x}(Eu_2O_3)_x$ ($0.01 \leq x \leq 0.10$ %mol) ceramic systems were investigated. The temperature and doping concentration dependences of the electrical conductivity were studied by four-point probe technique. The electrical conductivity increases with the increasing doping concentration and temperature. The highest value of the electrical conductivity is 0.013 $\Omega^{-1}cm^{-1}$ (x = 0.05, 750 ºC) for the β-phase at 670 ºC and 0.57 $\Omega^{-1}cm^{-1}$ (x=0.05, 800 ºC) in binary systems at 690 ºC. The phase transition which manifests itself by the jump in the conductivity curves was seen and verified by differential thermal analysis measurements. The activation energies of the samples were found to be about 0.71-1.57 eV.
Keywords: anionic conductors, bismuth oxide, ionic conductivity, four-point probe technique.

Resumo

Foi estudada a condutividade elétrica de sistema cerâmicos da fase β tetragonal $(Bi_2O_3)_{1-x}(Eu_2O_3)_x$ ($0,01 \leq x \leq 0,10$ mol%). A dependência da condutividade elétrica da temperatura e da concentração de dopantes foi estudada pela técnica das quatro pontas de prova. A condutividade elétrica aumenta com o aumento da concentração de dopantes e da temperatura. O maior valor da condutividade elétrica é 0,013 $\Omega^{-1}cm^{-1}$ (x = 0,05, 750 ºC) para a fase β a 670 ºC e 0,57 $\Omega^{-1}cm^{-1}$ (x = 0,05, 800 ºC) em sistema binários a 690 ºC. A transição de fase que se verifica pelo salto nas curvas de condutividade elétrica foi confirmada por medidas de análise térmica diferencial. As energias de ativação para as várias amostras está na faixa 0,71-1,57 eV.
Palavras-chave: condutores aniônicos, óxido de bismuto, condutividade iônica, técnica das quatro pontas de prova.

INTRODUCTION

Bismuth-based solid electrolyte systems are good oxygen anions conductors which have been extensively studied about electrical properties and structural properties [1-4]. Bi_2O_3-based materials are also used for the manufacturing of ceramic refractory, paint pigments, photovoltaic cells, oxygen sensors and oxygen pumps [5-7]. Many experimental researches have mostly focused on improving of the Bi-based electrolytes which have high oxide ionic conductivity at low temperatures and better performance in SOFC (Solid Oxide Fuel Cells). Because of their higher ionic conductivity, Bi_2O_3 polymorphs show better solid electrolyte property than well-known zirconium oxide type electrolyte systems [5-7]. Bi_2O_3 exhibits an extraordinarily rich phase polymorphism, denoted by α-Bi_2O_3 (monoclinic), β-Bi_2O_3 (tetragonal), γ-Bi_2O_3 (cubic, bcc), δ-Bi_2O_3 (cubic, fcc) ε-Bi_2O_3 (orthorhombic), ω-Bi_2O_3 (triclinic) and with two non-stoichiometric phases ($Bi_2O_{2.33}$ and $Bi_2O_{2.75}$) [8-10].

The stable or metastable occurrence of these phases depends on the conditions of thermal treatment and chemical doping/ alloying. δ-Bi_2O_3 is known as a high temperature stable phase which appears during the heating of pure α-Bi_2O_3 at ~730 ºC and it is stable up to melting point of Bi_2O_3 (825 ºC). Through the cooling of δ-Bi_2O_3 from high temperature to room temperature, a large thermal hysteresis effect is formed with the possible occurrence of two intermediate metastable β-phase or γ-phase. On the slow cooling, β-Bi_2O_3 occurs at around 650 ºC, whereas γ-form appears at ~640 ºC. Usually these metastable phases transform to α-phase below 500 ºC temperatures [8, 9, 11]. The δ, β and γ-phases of bismuth oxide can be stabilized by the addition of small amounts of other dopant M_2O_x type oxides such as M=V, Sb, La, Pr, Nd, Sm, Eu, Gd, Tb, Dy [2, 12, 13]. Several authors have tried what kind of dopant materials can make the increasing effect for the oxide ion conductivity of the Bi_2O_3-based electrolytes. Often the structure of the materials and doping processes play the important roles for the electrical conduction.

When the incorporating oxygen vacancies occur into their structures, they have an anionic conductivity character at which oxygen ions are the main mobile charge carriers. Usually larger amounts of M_2O_x dopant materials that introduce oxygen vacancies causes increasing the oxygen ionic conductivity of the Bi_2O_3-based electrolytic systems [8-10, 14]. The dopant type, stoichiometric ratio of the dopant, heating period, heat treatment temperature, cooling rate (slow cooling or quenching) and grinding time etc. are the major factors for the stabilization of the Bi_2O_3 polymorphs [15-18]. According to the our literature survey, doping of some lanthanide grouped oxide compounds which contain trivalent cation can make easer stabilization of β-phase and allow forming of the phase in the larger stoichiometric doping range. The difference in the ionic radius between the Ln and Bi atoms and doping concentration of Ln_2O_3 also cause to vary the oxygen ionic conductivity of the Bi_2O_3-based electrolyte system.

We have carried out this work in order to investigate the effects on the electrical conductivity of Eu_2O_3 doping in the Bi_2O_3 compound. In this study, we aimed more information about electrical conductivity properties of tetragonal phase. However, this study is different from the other studies because of its small dopant ratio. Electrical conductivity properties of the formed β-phase $(Bi_2O_3)_{1-x}(Eu_2O_3)_x$ binary systems in the range $0.01 \le x \le 0.1$ (ten different compositions) were investigated. Moreover, the possible reasons of the observed oxygen ionic conductions were discussed in the studied $(Bi_2O_3)_{1-x}$ – $(Eu_2O_3)_x$ binary system.

MATERIALS AND METHODS

For β-phase ceramic oxide mixtures reviewed in this work, which were synthesized by solid state reaction (SSR) method, description of the synthesis and processing conditions is found in previous publication [16]. For the total electrical conductivity (σ_T) measurements, tetragonal β-Bi_2O_3 samples were made on the agglomerated powders pressed at room temperature (diameter 13 mm, thickness ~0.5 mm) in a stainless steel die under ~1000 bar pressure. Disk-shaped pellets were sintered for 24 h in air at ~600 °C, then uncontrolled furnace cooling were made.

After heating at 600 °C, some X-ray diffraction (XRD) measurements showed that any phase change in the β-type samples was not observed. Scanning electron microscopy (SEM) revealed that the degree of densification in all cases ranged between 80 and 95%. The colour changes of the β-phase disk samples were determined carefully depending on the Eu_2O_3 additions and the heat treatment temperatures. The determination of crystal structure of samples was reported [16]. Tetragonal phases investigated in this study are seen in Table I.

The differential thermal analyses (DTA) were made in a simultaneous Perkin Elmer Diamond TG/DTA system. The specimens, usually 11.5 mg in mass, were heated at a rate of 10 °C.min^{-1} from room temperature to 700 °C. The measurements were made in dynamic atmosphere using

Table I - The observed phases in the $(Bi_2O_3)_{1-x}(Eu_2O_3)_x$ binary system.
[Tabela I - Fases observadas no sistema binário $(Bi_2O_3)_{1-x}$ $(Eu_2O_3)_x$.]

Synthesis Temperature (°C)	x (mol%)					
	2	3	4	5	6	7
750	-	β	β	β	β	-
800	β		β	β	β	β	β

a platinum sample holder and α-Al_2O_3 inert reference substance.

The electrical conductivities of the tetragonal samples were measured by using four-point probe dc method. For reducing contact resistance, fine platinum wires directly touched the surface of the samples. A special alumina kit was designed for the direct contacts of the wires and high temperature conductivity measurements (Fig. 1). Contact wires stay in wire holder and move up and down. When ring screw turns around itself, sample holder rise to contact wires. So samples strongly touch to wires. All of kit segments were fabricated by alumina. The ohmic character of the wire contacts was checked prior to the each measurement. The electric conductions were measured in the range between ~200 °C and ~700 °C with Keithley 2400 source meter and Keithley 2700 electrometer through an interface electronic card controlled by a computer. The temperature of the samples during these conduction measurements were determined by placing a K-type thermocouple 2-3 mm away from the sample. This thermocouple had a cold junction at 0 °C. The
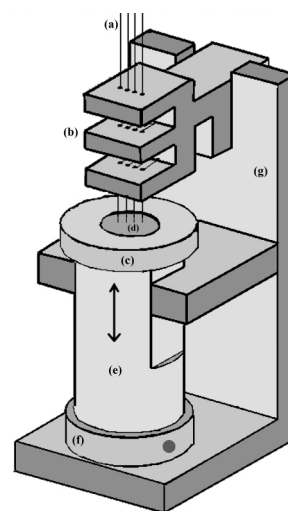

Figure 1: Four-probe electrical conductivity measurement kit; a) contact wires, b) wire holder, c) sample holder, d) sample, e) rising-descending body, f) ring screw, g) main body.
[Figura 1: Montagem para medida de condutividade elétrica pelo método das quatro pontas de prova: a) fios de contato, b) suporte do fio, c) porta-amostra, d) amostra, e) sistema para movimentação da amostra, f) anel com rosca, g) suporte.]

temperature increments during these measurements were kept smaller as the temperature approached to the phase transition temperature of substances. The conductivity and temperature measurements at each temperature were performed after thermal equilibrium had been reached.

The electrical conductivity was calculated using the below equation:

$$\sigma_T = G^{-1} \, I \, / \, V \qquad\qquad (A)$$

where G is the geometric resistivity correction factor. There is a functional relation between sample geometry and voltage and current values to determine the electrical conductivity. In the calculation of resistivity a correction factor, which varies with the sample geometry and the positions of contacts on the sample [19-25], should be used along with the V and I values [20, 21]. According to the sample dimensions t / s ≥ 0.5 and d / s < 40 when these ratios are considered, in the light of previous studies, G is obtained as [19-22, 26, 27].

$$G = 2.\pi.s.F_1.(t/s).F_2(d/s) \qquad\qquad (B)$$

In this expression:

$$F_1\left(\frac{t}{s}\right) = \frac{t/s}{2.\ln\left((\sinh(t/s)\,/\,(\sinh(t/2s)))\right)} \qquad (C)$$

$$F_2\left(\frac{d}{s}\right) = \frac{\ln 2}{\ln 2 + \ln\left[((d/s)^2 = (d/s)^2 - 3)\right]} \qquad (D)$$

where t is the thickness of the sample, d is the radius of the sample, s is the distance between the probes, F_1 and F_2 are additional correction factors.

RESULTS AND DISCUSSION

In our previous study we showed that the predominant phase has been tetragonal β-Bi_2O_3 in the $(Bi_2O_3)_{1-x}(Eu_2O_3)_x$ binary system (Table I) and the composition formula of the tetragonal solid solution was proposed as below [16]:

$$Bi(III)_{2-2x}Eu(II)_{2x}O_{3-x}\square_x \qquad\qquad (E)$$

where $\square$ symbolizes oxygen ion vacancy and x the value of the dopant ratio in Table I. Additionally, early workers reported that the β-Bi_2O_3 shows an oxygen deficiency type nonstoichiometry in the tetragonal lattice and its structural arrangements is nearly similar to the crystal structure of the cubic δ-Bi_2O_3, which has the defect fluorite type crystal structure and contains two O^{2-} vacancies in a per unit cell. Similarly, the pure β-phase includes two oxygen ion voids in the O^{2-} sublattices and its crystal formula is specified as

Bi_8O_{12}. The arrangements O^{2-} vacancies can be ordered or disordered in the tetragonal lattice according to the suggested crystal structure models [2, 10-12]. For that reason, the crystal formula of the formed β-phase was determined approximately depending on the calculated composition formula. As given below:

$$Bi(III)_{8-4x}Eu(II)_{4x}O_{12-2x}\square_{2+2x} \qquad\qquad (F)$$
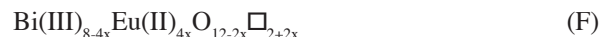
The crystal formula shows that the concentration of oxide anion vacancies increases with the increasing dopant concentration. This increasing of vacancy concentration also leads to raise the level of the non-stoichiometry of the produced solid solution. The results of the electrical conductivity measurement, which are discussed below, show a good agreement with the approximated crystal formula.

Fig. 2 shows the measured DTA curves of β-Bi_2O_3 doped with 6 mol% Eu_2O_3. The DTA curves of the other single β-phase samples were quite similar to the curve given in Fig. 2. On the DTA curve, a small endothermic peak is present in ~ 623 ºC. This peak was identified as due to the phase transition β-$Bi_2O_3 \rightarrow \delta$-$Bi_2O_3$ [11, 12, 19]. The DTA measurement indicated that the formed β-Bi_2O_3 type solid solution is thermally stable between room temperature and ~630 ºC.

In Fig. 3 and Fig. 4, the temperature dependence of the electrical conductivity ($\log \sigma_T - 1/T$) results for produced materials, which were doped with 2, 3, 5, 6 and 7 mol% Eu_2O_3 heat treatments at 750 and 800 ºC, are presented. For the other samples, the variations of the σ_T plots were quite similar to the given figures. These data were obtained under same heat treatment and at a constant heating rate in air.

The electrical conductivity of tetragonal type solid solution doped with Eu_2O_3 increases with the increasing temperature up to phase transformation temperature. Beyond this temperature the conductivity sharply increases with the increasing temperature up to ~750 ºC. A sharp increase in total conductivities was considered to be due to the phase transition of β-phase®δ-phase. These results
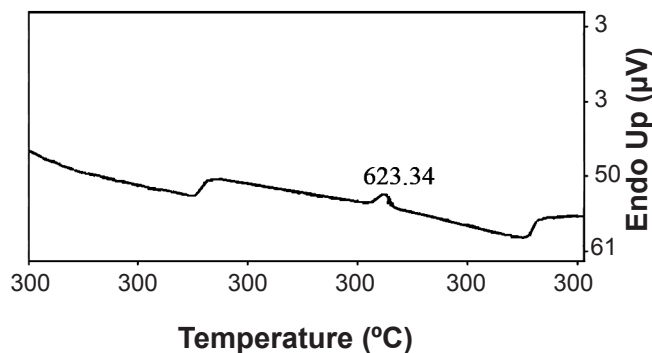

Figure 2: DTA curve of x = 0.06 molar doped $(Bi_2O_3)_{1-x}(Eu_2O_3)_x$ binary system synthesized at 750 ºC.
[Figura 2: Curva de análise térmica diferencial do sistema binário $(Bi_2O_3)_{1-x}(Eu_2O_3)_x$, x = 0,06 mol, sintetizado a 750 ºC.]
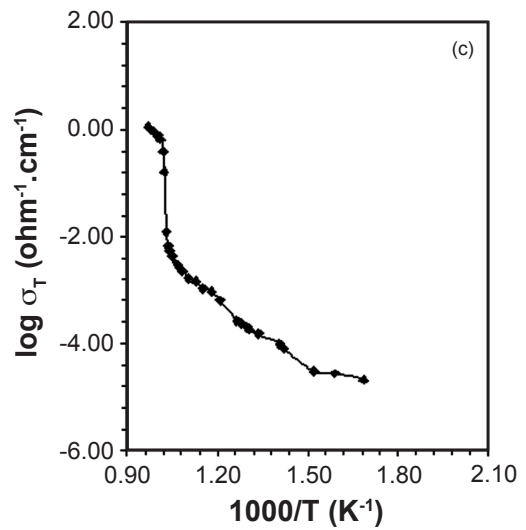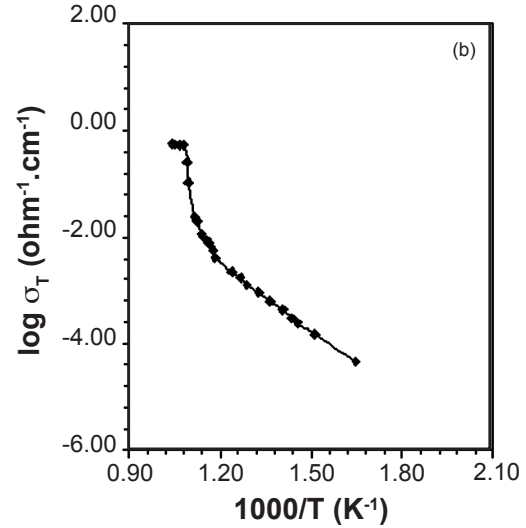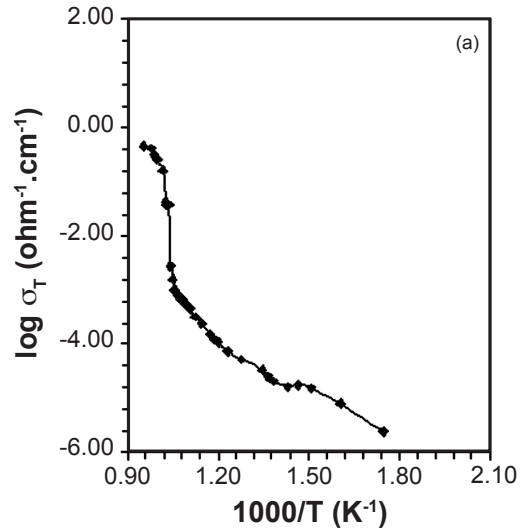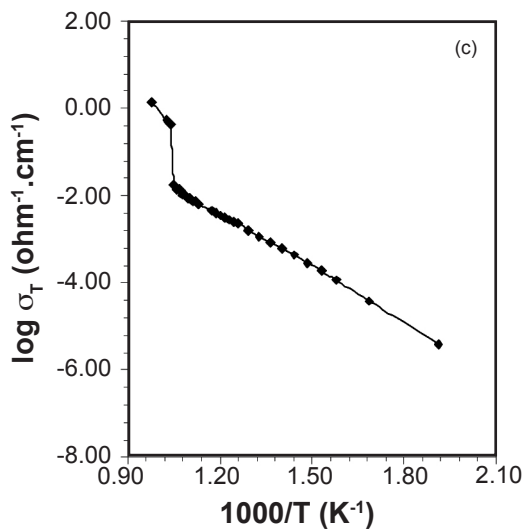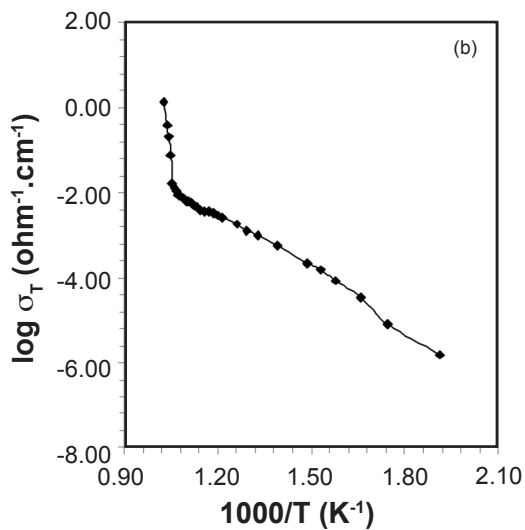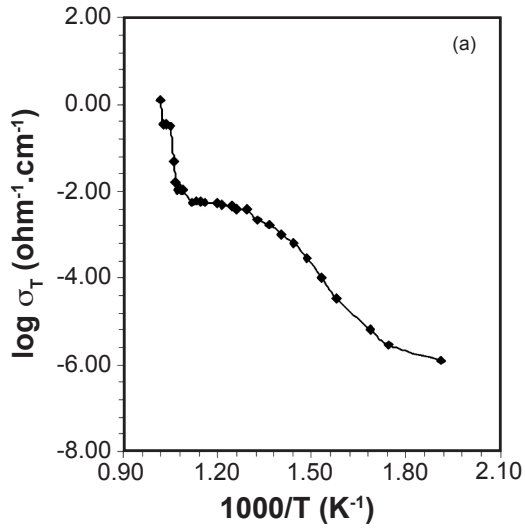
Figure 3: Arrhenius plots of the total electrical conductivity of the samples. (a) 3 mol%, (b) 5 mol%, (c) 6 mol% Eu_2O_3 doped Bi_2O_3 (750 °C, 48 h).
[Figura 3: Gráficos de Arrhenius da condutividade elétrica total das amostras Bi_2O_3 dopadas com x mol%Eu_2O_3 (750 °C, 48 h). (a) x = 3 (b) 5, (c) 6.]

Figura 4: Temperature dependence of the total electrical conductivity of the samples. (a) 2 mol%, (b) 5 mol%, (c) 7 mol% Eu_2O_3 doped Bi_2O_3 (800 °C, 48 h).
[Figura 3: Gráficos de Arrhenius da condutividade elétrica total das amostras Bi_2O_3 dopadas com x mol%Eu_2O_3 (800 °C, 48 h). (a) x = 2 (b) 5, (c) 7.]

have been also confirmed by the DTA measurements which are shown in Fig. 2. The formation of structural disorder during the phase transformation may also contribute to the improvement of ionic conductivity. A good agreement exists between our results and previous reports [28, 29]. Fig. 3 and Fig. 4 show that the conductivity of all samples increases with the increasing temperature. It was proposed that this is connected with the interstitial oxygen ionic migration which rises with the increasing temperature. At elevated temperatures, thermal vibration energy of the

O^{2-} ions causes higher oxygen ion movement rate which increases the conductivity level. Although the interstitial O^{2-} vacancies ($VO^{\bullet\bullet}$ = $\square$) are present in the crystal structure at low temperatures, the thermal energy of the charge carrier anions is not enough for jumping out of the interstitial $VO^{\bullet\bullet}$ positions. At low temperatures, the ordered structure of $VO^{\bullet\bullet}$ sub-lattice is dominant and a full randomization of the oxygen vacancies cannot occur. This structure causes a decay of the oxygen ionic mobility and lower electrical conductivity. At high temperatures thermal vibrations may also assist the jumping process momentarily by either shortening the jumping distances or by widening the jumping conducting paths through the crystal. On the other hand the degree of the disordered $VO^{\bullet\bullet}$ sublattice, which has a short-range ordering of oxygen vacancies along the some special directions of the tetragonal unit cell, may increases with the increasing temperature. This greater degree of the disorder defect lattice, especially with respect to the interstitial $VO^{\bullet\bullet}$, exhibits higher electrical conductivity.

The amount of doping has pronounced effects on the electrical conductivity of the samples. In Fig. 5 the mol% doping versus the maximum value of conductivity of β-phase was plotted.

The total electrical conductivity of Eu_2O_3 doped tetragonal type solid solution increases with the increasing europium ion substitution. In the composition region from $x = 0.03$ to $x = 0.09$ a continue jump in the Arrhenius plots appeared because the oxygen vacancies were confirmed to be in disordered structure. In most oxide-ion conductors the electrical conduction tends to increase with the increasing oxygen vacancy until the appearance of the association effect. The number of $VO^{\bullet\bullet}$ increases versus Eu_2O_3 content in this system. These experimental conductivity observations also agreed with the calculated crystal formula of the formed tetragonal type Bi_2O_3 electrolyte. As can be seen from the crystal formula (equation F), the concentration of $VO^{\bullet\bullet}$ increases with the europium content and so the ionic conductivity. This phenomenon was considered to be due to the reduction of the Eu^{3+} to Eu^{2+} and the oxidation of the host O^{2-} to O_2 molecule through the solid state reactions; as a result, the produced excess oxygen ions contribute to the ionic conduction. The oxidation half-reaction of the oxide ion is seen in the following chemical reaction:

$$O^{2-}(lattice) \rightarrow \square\,(VO^{\bullet\bullet}, \text{oxide ion vacancy}) + \qquad (G)$$
$$2e + 1/2\,O_2(g)$$

These reduction-oxidation reactions also indicated that the new $Eu^{2+} \leftrightarrow VO^{\bullet\bullet}$ electrostatic attractive forces should take place in the β-Bi_2O_3 crystal lattice, while substations between Eu and Bi cations. Moreover, the oxide ion mobility is depended upon the "free volume" of the unit cell through which ions migrate. The "free volume", defined as the difference between the tetragonal unit cell volume (as calculated from the unit cell parameters) and the total volume occupied by all the ions present within the unit cell (calculated from the effective ionic radii), tend to increase
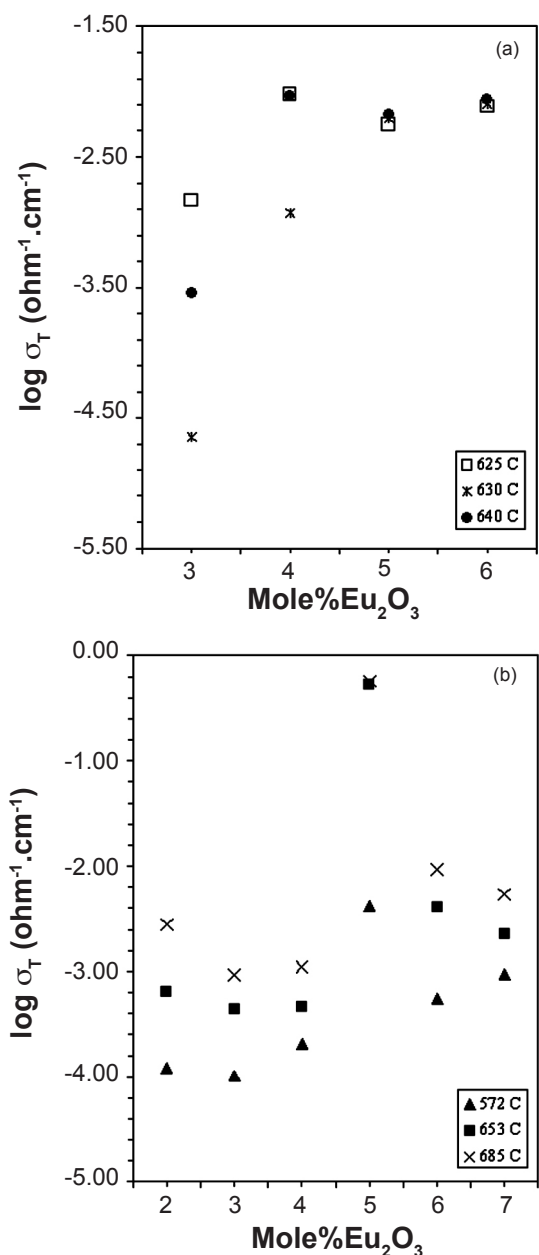

Figure 5: The effect of doping concentration on the electrical conductivity of the Eu_2O_3 doped β-phase samples synthesized at (a) 750 °C and (b) 800 °C.

[Figura 5: Efeito da concentração de dopante na condutividade elétrica total das amostras da fase β dopada com Eu_2O_3 sintetizadas a (a) 750 °C e (b) 800 °C.]

with the increasing Eu substitutions. As discussed in previous study [16], the lattice parameters and VO•• concentration of the obtained tetragonal type solid solutions increase with the Eu content. These results produce the rising of the free volume which initiates increasing the mobility of the oxygen ions and electrical conductivity.

Because $\log \sigma_T$ versus $1/T$ exhibits a linear relationship we decided that this behaviour of the electrical conductivity can be described by simple Arrhenius equation:

$$\sigma_T = \sigma_0 . \exp(-E_a/kT) \qquad (H)$$

where σ_0 the pre-exponential factor, E_a activation energy for the mobile oxygen ions (proportional to the slope) and k the Boltzmann constant. The Arrhenius conductivity curves have two regimes (Fig. 6).
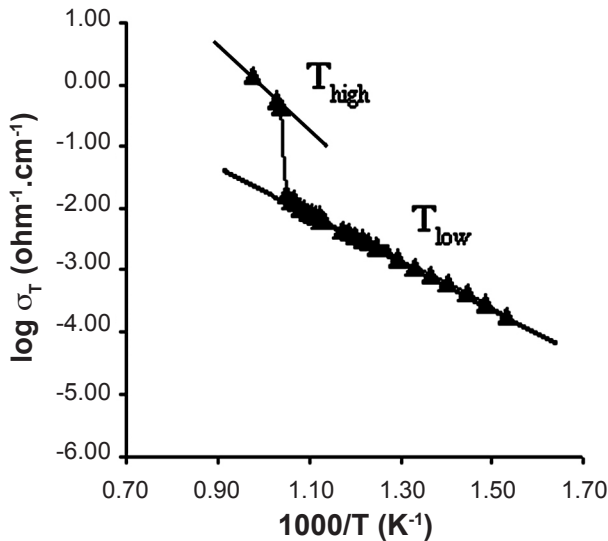

Figure 6: Two regimes of the Arrhenius plotc (x = 0.06, 750 °C).
[Figura 6: Dois regimes do gráfico de Arrhenius (x = 0,06, 750 °C).]

The activation energies are not similar at high and low temperature region due to the different conductivity mechanisms. This is a typical behaviour of Bi$_2$O$_3$-based solid electrolytes [29]. In the conductivity plots the low temperature regions belong to the stable tetragonal phase and the conductivity has changed as linear in this part of curves. Therefore, the activation energy E_a is stable in this temperature region and the conductivity mechanism is only one of its kind. The temperature ranges of the calculated E_a values are seen in Table II.

The calculated total values of the activation energy as a function of the mol% addition Eu$_2$O$_3$ are given in Table III.

It was found that the activation energy depended on the Eu$_2$O$_3$ content and was almost the same order as that of the other high oxide ion conductors. As can be seen in Fig. 7 the activation energy decreases slightly with increasing dopant concentration. There are some extreme deviations in 4 mol% (750 °C) and 3 and 6 mol% (800 °C). Except for these values, a decrease is observed in Fig. 7.

The decrease in E_a or the increase in σ_T is attributed

Table II - The temperature ranges of observed stable tetragonal phase.
[Tabela II - Faixas de temperatura da fase tetragonal observada.]

	Synthesis Temperature (°C)	
x (mol%)	750	800
2	-	560-675
3	300-530	585-690
4	380-580	490-650
5	590-700	415-605
6	340-620	515-685
7	-	490-670

Table III - The activation energy values of $(Bi_2O_3)_{1-x}(Eu_2O_3)_x$ binary system.
[Tabela III - Valores de energia de ativação do sistema binário $(Bi_2O_3)_{1-x}(Eu_2O_3)_x$.]

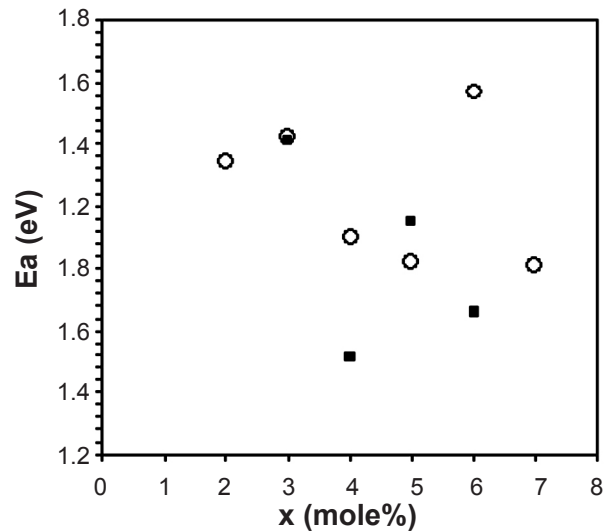| Synthesis temperature (°C)	x (mol%)	E_a (eV)
	3	1.41
750	4	0.71
	5	1.16
	6	0.86
	2	1.34
	3	1.42
800	4	1.10
	5	1.02
	6	1.57
	7	1.01

Figure 7: Dopant content dependence of the activation energy (Sintered at ■; 750 °C and ¤; 800 °C).
[Figura 7: Dependência da energia de ativação com o teor de dopante (Sinterizado a ■; 750 °C and ¤; 800 °C).]

to an order/disorder transition of the oxygen vacancies at high temperatures or high doping additions. The calculated values E_a from the Arrhenius plot indicate that the disorder arrangement of the interstitial oxygen vacancies becomes a major effect in high doping compositions. The decrease in total E_a is due to the increase in concentration of charge compensating O^{2-} vacancies and the conducting species in this tetragonal Bi_2O_3-based electrolyte. This ensuing increase in the conductivity with the increasing dopant concentration is due to the disorder of the anion sublattice. This disorder structure can occur partly because of the concentration of $VO^{\bullet\bullet}$ should be not higher than the solubility limit. Because of their different positive oxidation numbers, the degree of electrostatic attraction forces and difference in cationic radius, the weaker $Eu^{2+} O^{2-}$ and $Eu^{2+}\leftrightarrow VO^{\bullet\bullet}$ bonds should occur in the disordered crystal structure compared to the that of $Bi^{3+}\leftrightarrow O^{2-}$ and $Bi^{3+}\leftrightarrow VO^{\bullet\bullet}$ bonds whereas substation of Eu ions with Bi cations (Eu-O bond is longer than Bi-O bond). Therefore, $VO^{\bullet\bullet}\leftrightarrow VO^{\bullet\bullet}$ repulsions and the dopant vacancy interactions ($Eu^{2+}\leftrightarrow VO^{\bullet\bullet}$) should have a higher statistical probability of occurrence.

These dopant-vacancy associated defects and the formed weaker Coulombic $Eu^{2+}\leftrightarrow VO^{\bullet\bullet}$ attractions should be responsible for the variation of E_a values with the dopant concentration. On the other hand the total activation energy for ionic conductivity is expressed by [30, 31]:

$$E_a = E_m + E_d \qquad (I)$$

where E_m is the migration activation energy for jumping interstitial O^{2-} ions to the correct O^{2-} vacancy positions and E_d is the additional energy required to break up the defect associates As a general rule, E_d shows a decrease with the increasing ionic radii of the dopant cation [30, 31]. It was determined that this rule agreed with our considerations. E_m is directly related to the mobility (μ) of the oxygen ions which is dominated by the following Nernst-Einstein equation [30, 31]:

$$\mu = D.Z.e/kT \qquad (J)$$

where D, Z, e are the O^{2-} diffusion coefficient, the valence number of the carrier, and the elementary electric charge, respectively. Therefore, the O^{2-} ionic mobility can be expressed by:

$$\mu = (Z.e/kT).D_0.\exp(-E_m/kT) \qquad (K)$$

Moreover, the total oxide ionic conduction is expressed as follows:

$$\sigma_T = 2.n.e.\mu \qquad (L)$$

where n is the carrier density of the mobile oxide ions. It was aimed that another reason of decreasing in the E_a with increasing Eu substitution is due to the weaker Eu–O bond

compared to that of Bi–O and increasing concentration of the oxygen vacancies. The migration activation energy E_m for the interstitial oxide anions through the tetragonal Bi_2O_3 lattice is dependent upon both the oxygen binding energy in the lattice and the "free volume" through which O^{2-} ions migrate, i.e., E_m is the sum of the energy required to break a lattice cation-oxygen bond and an energy term dependent on the oxide ion mobility between the interstitial O^{2-} vacant lattice sites. The decreasing the cation-oxygen bond energy causes dropping on the E_m and E_a values which was observed minimum E_a value and maximum electrical conductivity.

CONCLUSIONS

The results of DTA measurements are consistent with the results of the electrical conductivity observations. In the diffusion mechanism of Eu ions into Bi_2O_3 the reduced europium cations are substituted bismuth cations in the tetragonal crystal lattice. During these replacements between the dopant and host cations the O^{2-} ions in the structure have been oxidized to O_2 molecules. The heat treatments of the $(Bi_2O_3)_{1-x}(Eu_2O_3)_x$ binary system are responsible for forming O^{2-} vacancies, which showed disordered structure. The higher doping rates of Eu_2O_3 introduce more distorted defects into the structures and the most predominant defects are oxygen vacancies, which increase with the increasing amount of Eu_2O_3. The measured conductivity increases with the increasing of Eu_2O_3 content and temperature. Furthermore, the increasing dopant concentration also causes the stabilization of the disordered structure for the oxygen vacancies and decreases the activation energy.

ACKNOWLEDGEMENTS

REFERENCES

[1] O. Turkoglu, I. Belenli, J. Therm. Anal. Calorim. **73** (2003) 1001.
[2] P. Millan, J. M. Rojo, A. Castro, Mater. Res. Bull. **35** (2000) 835.
[3] M. Yashima, D. Ishimura, Chem. Phys. Lett. **378** (2003) 395.
[4] V. Fruth, A. Ianculescu, D. Berger, S. Breda, G. Voicu, E. Tenea, M. Popa, J. Eur. Ceram. Soc. **26** (2006) 3011.
[5] N. M. Sammes, G. A. Tompestt, H. Nafe, F. Aldinger, J. Eur. Ceram. Soc. **19** (1999) 1801.
[6] T. Takahashi, H. Iwahara, Y. Nagai, J. Appl. Electrochem. **2** (1972) 97.
[7] S. Nakayama, Ceram. Int. **28** (2002) 907.
[8] H. A. Harwig, J. W. Weenk, Z. Anorg. Allg. Chem. **444** (1978) 167.
[9] H. A. Harwig, A. G. Gerards, Thermochim. Acta **28**

(1979) 121.

[10] M. Drache, P. Roussel, J. P. Wignacourt, Chem. Rev. **107** (2007) 80.

[11] J. W. Medernach, R. L. Snyder, J. Am. Ceram. Soc. **61** (1978) 494.

[12] M. Miyayama, S. Katsuta, Y. Suenaga, H. Yanagida, J. Am. Ceram. Soc. **66** (1983) 585.

[13] M. Drache, S. Obbade, J. P. Wignacourt, P. Conflant, J. Solid State Chem. **142** (1999) 349.

[14] H. A. Harwig, A. G. Gerards, J. Solid State Chem. **26** (1978) 265.

[15] O. Turkoglu, A. Gumus, I. Belenli, Bal. Phys. Lett. **6** (1998) 34.

[16] O. Turkoglu, M. Soylak, I. Belenli, Bull. Mater. Sci. **25** (2002) 583.

[17] O. Turkoglu, M. Soylak, Asian J. Chem. **14** (2002) 3.

[18] O. Turkoglu, F. Altiparmak, I. Belenli, Chem. Pap. **5**, 57 (2003) 304.

[19] F. M. Smits, Bell Syst. Tech. J. **37** (1958) 711.

[20] M. P. Albert, IEEE Trans. Electron. Devices **11** (1964) 148.

[21] L. J. Swartzendruber, Solid State Ionics **7** (1964) 413.

[22] D. E. Vaughan, Brit. J. Appl. Phys. **12** (1961) 414.

[23] M. Yamashita, Jpn. J. Appl. Phys. **26** (1987) 1550.

[24] M. Yamashita, Jpn. J. Appl. Phys. **27** (1988) 1317.

[25] L. B. Valdes, Proc. IRE **42** (1954) 420.

[26] D. K. Schroder, *Semiconductor Material and Device Characterization*, 3th Ed., John Wiley & Sons, New Jersey, USA (2006) p. 8.

[27] S. Yilmaz, *Synthesis Characterization and Investigation of the Solid State Oxygen Ionic Conductivities of β-Bi$_2$O$_3$ Type Solid Electrolytes Doped with Dy$_2$O$_3$, Eu$_2$O$_3$, Sm$_2$O$_3$*, Ph.D. Thesis, Gazi University, Ankara, Turkey (2008) p. 68.

[28] S. Yilmaz, O. Turkoglu and I. Belenli, Res. Lett. Mater. Sci. (2007) 5 p., doi:10.1155/2007/97204.

[29] S. Yilmaz, O. Turkoglu and I. Belenli, Mater. Chem. Phys. **112** (2008) 472.

[30] R. West, Basic Solid State Chemistry, John Wiley & Sons, Chichester, UK (1988) p. 300.

[31] C. Kittel, Introduction to Solid Satate Physics, John Wiley & Sons, New York, USA (2005) p. 585.